

DOI: https://dx.doi.org/10.54203/jceu.2025.8

## Seismotectonics and Earthquake Hazards of the Coastal Aegean **Region: A Regional Assessment**

Korkmaz Yıldırım 🚾 🗓

Aydın Adnan Menderes University, Aydın Vocational School, Efeler/Aydın, Türkiye

Corresponding author's Email: kyildirim@adu.edu.tr

#### **ABSTRACT**

This study comprehensively examines the seismotectonic characteristics of the Coastal Aegean Region and evaluates earthquake hazard probabilities based on historical, structural, and geodynamic data. Western Anatolia and the Coastal Aegean Region represent high-seismic-risk zones characterized by a complex deformation regime, where both normal and strike-slip faults are actively influential. The research investigates local fault systems in various segments, including İzmir, Balıkesir, Aydın, Muğla, Gökova, Skyros, and Sığacık. GPS measurements, microseismic records, tomographic analyses, and field observations were integrated to perform seismic hazard assessments. The vulnerability of traditional structures and the influence of local soil conditions on structural performance were also evaluated, supported by empirical and seismic hazard analysis results. Findings indicate that the seismic hazard in the region is associated not only with major faults but also with micro-scale stress accumulation and structural weaknesses. The magnitudes, locations, and characteristics of historical earthquakes were found to be consistent with the results of seismic hazard analyses. In this context, measures such as microseismicity monitoring, tsunami and earthquake early warning systems, and the reinforcement of building stock are projected to play a significant role in reducing disaster risk.

Keywords: Seismotectonics, Earthquake hazard assessment, Coastal Aegean Region, Fault systems, Structural vulnerability

#### INTRODUCTION

Turkey and its surrounding geographical region are located along the Alpine-Himalayan belt, one of the most active tectonic zones in the world. This tectonic setting has been responsible for numerous destructive earthquakes throughout history (Denli, 2018). This active tectonic environment is highly complex in terms of both plate boundary characteristics and microplate dynamics (Müller et al., 2013). The Aegean region, located in western Turkey, lies within the interaction zone of both continental and marine tectonic regimes. In particular, the segments of the North Anatolian Fault extending into the Aegean Sea and the subduction zone developed along the Hellenic Arc are among the primary sources of seismic activity in this area (Papanikolaou et al., 2019; Müller et al., 2013).

The Aegean region is characterized by a complex deformation regime that is not confined solely to plate boundaries but also involves microtectonic movements. graben structures, and numerous surface faults (Seyrek, 2020). Within this framework, settlement areas such as Muğla, Aydın, İzmir, and their surroundings are among

the regions with high earthquake risk. Local soil conditions, the state of the building stock, and the vulnerability of the historical urban fabric further exacerbate potential disaster scenarios (Aktaş et al., 2022). Furthermore, the earthquake that struck the Aegean Sea-İzmir region on 30 October 2020 served as a stark reminder that the region's earthquake-generating potential is not only a scientific reality but also a pressing social reality (Triantafyllou et al., 2021; Aktaş et al., 2022).

The aim of this study is to conduct a detailed examination of the complex seismotectonic framework outlined above, to understand the seismicity dynamics of specific areas (e.g., İzmir, Muğla, Aydın, Balıkesir, and the Coastal Aegean), and to evaluate earthquake activity and associated risks from both geoscientific and structural perspectives on a regional scale. Furthermore, by integrating extensive historical datasets with a broad body of literature, contemporary observational techniques, and seismic hazard analyses, this study seeks to provide a comprehensive scientific framework for assessing

Revised: September 20, 2025 Received: August 18, 2025

RESEARCH ARTICLE

potential earthquake activity and associated risks in the Coastal Aegean section of the Aegean Region.

Scientific understanding of occurrence, distribution, and impacts of earthquakes has advanced through the integration of multidisciplinary studies. In the context of Turkey and specifically the Aegean region, geological, geophysical, seismological, and engineeringbased research aimed at understanding seismotectonic structures has been ongoing for decades. Early studies, particularly those focusing on the western extensions of the North Anatolian Fault Zone (NAFZ) and the active fault zones in the Aegean Sea, have provided significant insights into both the tectonic regime and faulting characteristics of the region (Müller et al., 2013; Papanikolaou et al., 2019).

GPS measurements and stress field modeling have made significant contributions to understanding the dynamics of the transition zone between the motion of the Aegean microplate and the North Anatolian Fault (Briole et al., 2021; Müller et al., 2013). These studies have revealed that, in addition to northeast—southwest trending right-lateral strike-slip faults, normal faulting components are also active in the region. In particular, kinematic data derived from both extension directions and fault-plane solutions around the Northern Aegean, Skyros, and the Sporades Islands confirm the presence of multi-directional deformation processes (Papanikolaou et al., 2019; Müller et al., 2013).

Turkey is located at the convergence zone of the Eurasian, Arabian, and African plates, resulting in a highly complex tectonic framework. As a consequence of these plate interactions, three primary tectonic regimes are observed in the country: the North Anatolian Fault Zone (NAFZ), characterized by east—west compression and right-lateral strike-slip motion; the East Anatolian Fault Zone (EAFZ), defined by left-lateral strike-slip motion; and the extensional regime dominating the western Aegean region (Müller et al., 2013; Briole et al., 2021).

The North Anatolian Fault Zone (NAFZ), located in northern Turkey, is one of the most active and seismically significant fault systems in the region, extending approximately 1,500 km in length. This fault zone progresses from the northeast to the southwest, reaching the Sea of Marmara and continuing toward the Aegean Sea through offshore segments (Müller et al., 2013; Papanikolaou et al., 2019). Along this zone, a right-lateral slip rate of approximately 20–25 mm per year has been documented (Briole et al., 2021).

To the south, the East Anatolian Fault Zone (EAFZ) is another major strike-slip fault system, developed as a result of the northward movement of the Arabian Plate. This fault system, which dominates eastern Turkey, together with the associated compressional regime, plays a key role in shaping the overall deformation dynamics of the country. Between the NAFZ and EAFZ lies Central Anatolia, a relatively stable tectonic block (Briole et al., 2021). In contrast, western Turkey is characterized by an extensional tectonic regime, differing from the compressional framework observed in the east. This transitional zone is distinct from other parts of the country in terms of both faulting style and seismotectonic behavior.

In conclusion, the literature emphasizes the necessity of evaluating a wide range of variables at both macro scales (plate motions, fault systems) and micro scales (soil profiles, building types). Studies conducted in the Aegean region demonstrate how this holistic approach is reflected in the field and form the theoretical basis of the present research.

#### Seismotectonics of the Aegean Region

The Aegean Region, located at the westernmost part of Turkey, is directly influenced by the Aegean microplate. This microplate moves southwestward at an approximate rate of 30 mm/year relative to the Eurasian Plate (Müller et al., 2013; Briole et al., 2021). This motion has resulted in an extensional tectonic regime in which normal faulting is predominant. The regime is particularly evident in the graben systems, such as the Gediz and Büyük Menderes grabens. Much of the deformation in the Aegean Region is attributed to north—south extensional movements, a phenomenon confirmed by GPS measurements. Areas such as the Gulf of İzmir, Gökova, Skyros, the Gulf of Sığacık, and the vicinity of Kuşadası are characterized by high deformation rates (Papanikolaou et al., 2019; Triantafyllou et al., 2021).

Another outcome of this tectonic regime is the frequent occurrence of shallow-focus earthquakes. The Mw 7.0 Samos earthquake of 30 October 2020 is a product of this extensional tectonic setting and exhibits the characteristics of normal faulting (Triantafyllou et al., 2021). This event once again demonstrated the earthquake-generating potential of the active faults in the eastern part of the Aegean Sea. Furthermore, structures such as the Skyros Basin exhibit both right-lateral and normal faulting components, as a result of the westward propagation of the North Anatolian Fault (Papanikolaou et al., 2019). This combination renders the tectonic evolution of the region highly complex and multidimensional. Overall, the seismotectonic framework of the Aegean

Region is shaped by dynamics that differ from those in other parts of Turkey. This distinction is clearly reflected in both fault geometries and earthquake behavior, making the Aegean one of the most unique regions of the country in seismological terms.

## Regional and Event-Based Analyses

# The Mediterranean, the Hellenic Arc, and the Subduction Process

The Eastern Mediterranean hosts an active subduction zone formed by the northward movement of the African Plate beneath the Eurasian Plate. The most prominent geotectonic structure of this zone is the Hellenic Arc. along which seismic events render the eastern Mediterranean tectonically hazardous (Papanikolaou et al., 2019; Triantafyllou et al., 2021). The westward escape of the Aegean microplate induces extensional faulting along the Hellenic Arc. This extensional regime has generated active fault systems both on the seafloor and in their onshore continuations. Contemporary research also shows that submarine landslides provide a secondary contribution to such seismic events (Triantafyllou et al., 2021). Studies based on potential field data and local crustal structure reveal the presence of an extensive fracture system along the Mediterranean, predominantly characterized by normal faulting, and indicate the dominance of an extensional tectonic setting (Seyrek, 2020; Müller et al., 2013). Collectively, these features demonstrate that the region constitutes an active geodynamic zone that must be closely monitored for both earthquake and tsunami hazards.

### Northwestern Anatolia, Manisa, Balıkesir, and Kütahya

Northwestern Anatolia is one of the most seismotectonically active regions in Turkey, influenced by both the North Anatolian Fault Zone (NAFZ) and the Aegean extensional regime. Earthquakes in this region are associated with both right-lateral strike-slip faulting and extensional structures (Seyrek, 2020). The western branches of the NAFZ, after crossing the Sea of Marmara, merge with numerous surface faults in and around Balıkesir, forming a complex tectonic network. The Balıkesir Plain contains subsidence basins bounded by active normal faults from the neotectonic period, which frequently generate small- to moderate-magnitude earthquake. Geological studies in the area indicate that the Balıkesir faults are young and active, as evidenced by surface morphotectonic features. Structural deformations along these predominantly east-west trending faults contribute significantly to the seismic hazard of the region (Tağıl, 2004).

Kütahya and its surroundings are affected both by the southern branches of the NAFZ and by deep fault systems extending toward the Central Anatolian Plateau. Seyrek (2020), in an evaluation conducted for the new Turkey Seismic Hazard Map, reported that the Kütahya region possesses high acceleration potential, with local soil conditions having a substantial impact on design spectra. Historically, the region has experienced destructive earthquakes, including the 1919 Balıkesir, 1944 Ayvalık, and 1970 Kütahya events (KOERİ, 2020, Eastern Aegean Sea Earthquake, Press Bulletin). These earthquakes caused severe damage to both the urban fabric and infrastructure (Denli, 2018), underscoring the region's high hazard potential based on both historical and contemporary data.

## Southwestern Anatolia: Muğla, Gökova, Marmaris, and Fethiye

Muğla and its surroundings, located in the southwestern corner of Turkey, represent a critical area in terms of both seismotectonic diversity and high earthquake hazard. This region is characterized by the Gökova Graben System, one of the westernmost extensions of the Aegean extensional regime (Sezer, 2003). The faults extending along the Gulf of Gökova are oriented east—west and predominantly exhibit normal faulting characteristics. Studies conducted in the Marmaris and Yeşilova areas have indicated that these faults have the potential to produce surface ruptures and have caused significant seismic events in the past (Yildirim, 2016). Notably, the earthquakes that occurred in Muğla in 2004 demonstrated that the region is densely cut by active faults, many of which are traceable at the surface.

The Muğla seismotectonic province, together with its immediate surroundings, covers the area between latitudes 26.00°-30.00°E. 36.00°-37.50°N and longitudes Geologically and morphotectonically, this seismotectonic province occupies a place within the Alpine Belt, which extends from the Azores Islands to Indonesia. The Muğla earthquake zone is controlled by the Western Anatolian extensional regime, which includes the Aegean-Hellenic Trench and its eastern continuation, the Cyprus Arc, as well as the Aegean graben system. This region constitutes an active graben belt where normal faulting is widespread, resulting in frequent shallow-focus earthquakes (Anadolu Kılıç,2017). The earliest available record of an earthquake in the Muğla region, according to USGS-NEIC (U.S. Geological Survey–U.S. National Earthquake Information Center) data, is of Greek origin and dates back to 411

B.C., corresponding to a surface-wave magnitude (Ms) of 7.0, in the Güllük (Kerme) Gulf area. Earthquakes with magnitudes of 7.2 Ms (227 B.C.), 7.0 Ms (197 B.C.), and 7.0 Ms (183 B.C.) occurred in the vicinity of Rhodes Island. According to USGS–NEIC data compiled from NASA–NOAA sources, the largest recorded earthquake in this region was the 27 August 1886 Bodrum earthquake, with a magnitude of 8.39 Ms.

Significant events include a 1926 earthquake in Muğla; the 13 December 1941 Dağpınar-Muğla earthquake (M 6.5); the 24-25 April 1957 Fethiye earthquakes (M 6.2 and M 7.1); and the 20 July 2017 Gökova Gulf–Mediterranean earthquake (M 6.6) (KOERİ, 2020, Eastern Aegean Sea Earthquake, Press Bulletin). The 1957 Fethiye earthquake caused severe damage to buildings in Fethiye. The shocks also inflicted substantial destruction on structures in Eskihisar Village (Yatağan), Marmaris, Milas, Solmaz Village (Tavas), and the Kalkan district of Kaş. Approximately 60% of the houses in Marmaris were completely destroyed, while 80% of the buildings in Cameli became uninhabitable. On 26 April, 15 additional houses collapsed in Solmaz Village. In Eskihisar Village, 300 out of 320 households were destroyed (Aslan, 2017). Given the prevalence of traditional settlements in this area, the building stock poses a significant seismic risk. In this context, Southwestern Anatolia is a region that requires a multidisciplinary disaster risk management approach, taking into account both geoscientific data and structural performance.

#### **İzmir and Surroundings**

İzmir and its surrounding areas are among the most densely populated and seismotectonically complex regions in western Turkey. The region lies at the intersection of east—west trending normal faults, northeast—southwest oriented right-lateral strike-slip faults, and active graben systems. This complex structure has been examined in detail using both geological and seismological data, and active faults located directly beneath the city have been identified (Kılıç, 2006).

The İzmir Fault and other parallel fault systems are particularly concentrated in the Seferihisar and Balçova areas. Morphometric analyses conducted on these faults have revealed that fault segments such as the Gümüldür segment possess both normal and strike-slip components (Yerli et al., 2021). This kinematic characteristic of the faults increases the risk of surface rupture, especially when combined with strike-slip effects in destructive earthquake scenarios. In light of these data, it is clear that İzmir is at high earthquake risk not only because of its proximity to

active faults but also due to its complex subsurface structure.

### Northern Aegean, Sığacık, Skyros, and the Skyros Basin

The Northern Aegean region is a microplate boundary with high seismic activity, developed under the influence of both the strike-slip fault systems in Western Anatolia and the Aegean extensional regime. This area is defined as one of the transition zones where both normal and strikeslip faulting occur together (Müller et al., 2013). The Skyros Basin is located in the eastern part of the Northern Aegean and is identified as an active deformation zone. The development of this basin emerged as a result of the westward extension of the North Anatolian Fault and was also shaped by extensional forces originating from the Hellenic arc system (Papanikolaou et al., 2019). GPS measurements indicate that extensional deformation of up to 20 mm per year is observed in this region, and that the Skyros Basin is under an active normal faulting regime (Müller et al., 2013).

One of the significant earthquakes in Skyros and its surroundings is the Mw 6.4 event that occurred in 2001 near Skyros Island. This event demonstrated that the faults in the region are not purely normal faults but may also have right-lateral components (Ganas et al., 2005). The same study emphasizes that stress fields developing in different directions lead to variations in local stress orientations in the region. The Gulf of Sığacık, located along the Turkish coast, is defined by active faults extending off Seferihisar, west of İzmir. This area drew attention with a series of successive earthquakes in 2005, during which it was determined that the faults exhibited both strike-slip and normal components (Benetatos et al., 2006). Seismic sequence analyses revealed that the faulting style is right-lateral with a vertical component, reflecting the complex tectonic regime in the region. These two areas—the Skyros Basin and the Gulf of Sığacık—are key focal points in regional seismic hazard assessments due to both their active faulting and their proximity to coastal cities.

#### Microseismicity and GPS

The tectonic complexity of the Aegean Region is highlighted not only by large earthquakes but also by the persistent occurrence of low-magnitude seismic activity—microseismicity—throughout the area. Microseismic activity provides an important dataset, particularly along fault zones, indicating stress accumulation and the distribution of structural weaknesses (Müller et al., 2013). Another method used to understand stress orientations is

stress tensor inversion analysis. Studies conducted in the Aegean Region and in the western segments of the North Anatolian Fault extending into the Aegean Sea have shown that the westward escape of the Anatolian block, combined with north–south extension, produces stress heterogeneity in the region (Ganas et al., 2005). This heterogeneous stress field also explains the variable kinematic characteristics of regional faults.

GPS data quantitatively reveal the deformation rates of the region and enable the development of block models. In the study by Briole et al. (2021), it was determined that average strain rates in the Aegean Region can reach up to 20 mm/year, with the most intense deformation occurring in the Gulf of İzmir, Southwestern Aegean, and Eastern Aegean Islands. The same study identified the boundaries between crustal blocks, highlighting zones where seismic coupling is stronger. In conclusion, when microseismicity data are evaluated together with GPS observations, it becomes clear that the Aegean Region has a highly active and heterogeneous tectonic regime not only at the surface but also at depth within the Earth's crust.

#### MATERIAL AND METHOD

The size-frequency distribution of many geological and geophysical variables exhibits a fractal character and can be described by scaling laws. Phenomena observed in tectonic processes—such as fracturing, faulting, and seismicity—also reflect this scale invariance and self-similarity.

The statistical distribution of earthquakes was first expressed through the power law formulated by Gutenberg and Richter. The Gutenberg–Richter law serves as a fundamental tool in the statistical analysis of earthquake catalog data and is widely used in regional seismic hazard assessments, fault zone characterization, and earthquake probability estimation. Moreover, temporal and spatial variations of the b-value provide important insights into the monitoring of seismic cycles and the potential forecasting of large earthquakes (Pardo-Igúzquiza and Dowd, 2024).

All earthquake records for the Coastal Aegean region were obtained from the earthquake catalogs provided by the Kandilli Observatory, the Disaster and Emergency Management Authority (AFAD), and the United States Geological Survey (USGS). The catalogs were queried for the period 1900–2024, using the latitude range  $36.90^{\circ}$  N –  $40.50^{\circ}$  N and the longitude range  $26.00^{\circ}$  E –  $29.50^{\circ}$  E for the Coastal Aegean. Within these coordinates, the dataset

covers İzmir, Aydın, Muğla, Manisa, Balıkesir, and Çanakkale provinces, as well as parts of Denizli, Uşak, and Bursa, enabling detailed data collection.

All data from the Kandilli Observatory, AFAD, and USGS were combined and categorized by year, moment magnitude (Mw), location, and depth, resulting in a total of 178,628 earthquake events. In seismic risk analyses, a lower magnitude threshold (Mc) is typically defined. Earthquakes with magnitudes smaller than 4 generally do not cause damage to engineering structures, and the data for such events are often unreliable (Kalyoncuoğlu et al., 2006). Since measurements and earthquake catalogs from earlier years are not as precise as modern data, a threshold of Mc < 5 was selected in this study to ensure statistical significance.

The most widely known equation for magnitude—frequency distribution is the Gutenberg-Richter relationship (Kalyoncuoğlu et al.2006,).

$$Log N(M) = a - bM$$
 (1)

Where, *N* represents the number of earthquakes for a given magnitude *M*, while "a" and "b" are constant regression coefficients. The "a" coefficient, which depends on the size of the study area and the observation period, is related to the level of seismic activity (the earthquake productivity of the crust). The "b" coefficient, which is inversely proportional to crustal stress, is defined as a parameter associated with the physics of earthquake occurrence (Anadolu Kılıç and Kalyoncuoğlu, 2017). After these constants are determined using the Least Squares Method (LSM), the recurrence interval for a target magnitude in the study area is calculated using the following formula (Anadolu Kılıç and Kalyoncuoğlu, 2017).

$$TR = \Delta T / 10(a - bMh) \tag{2}$$

Here,  $\Delta T$  represents the time span covered by the seismicity catalog (or the observation period, Tg). In the statistical risk analysis, the annual risk for a given magnitude M is calculated by determining the probability of occurrence of earthquakes with magnitudes equal to or greater than M on a yearly basis (Yildirim, 2016). The probability (%) of the target earthquake occurring within a specific future time period T is calculated using the formula presented in Equation 3.

$$R=1-e-N(Mh)T \tag{3}$$

Here, R(M) denotes the seismic hazard (seismic risk), n(M) represents the annual number of earthquakes, and T refers to the future period under consideration. For the data obtained from the Kandilli Observatory, the probabilities of earthquakes with magnitudes equal to or greater than a given M are calculated using Equation 3.

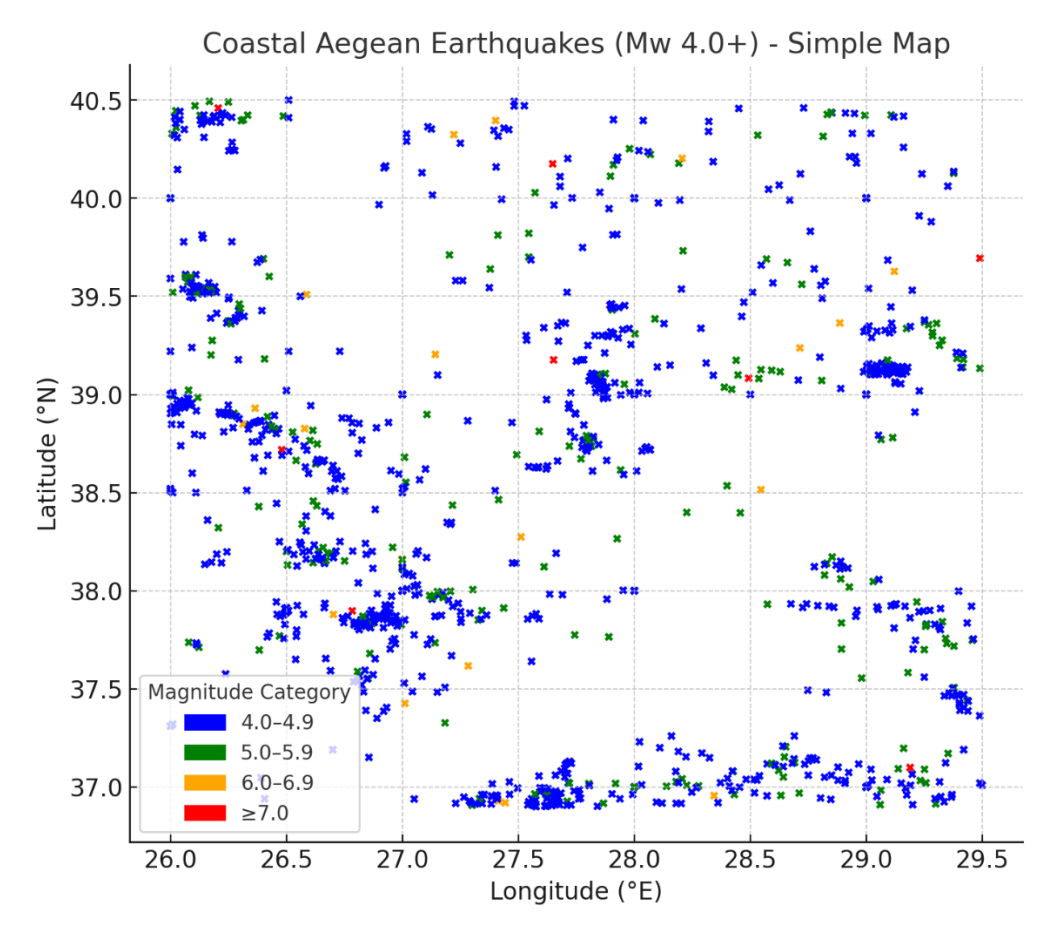


Figure 1. Earthquake map of the Coastal Aegean region.

#### **RESULTS**

All earthquake data for the period 1900–2025 were obtained from the Kandilli Observatory, and the number of earthquakes by intervals is presented in Table 1.

**Table 1**. Number of earthquakes between 1900 and 2025

Magnitude Range	Number of Earthquakes (N)				
3.5-3.9	2102				
4.0-4.4	597				
4.5-4.9	323				
5.0-5.4	124				
5.5-5.9	28				
6.0-6.4	5				
6.5-6.9	6				
7.0-7.4	3				

As shown in Table 1, the number of earthquakes is inversely proportional to magnitude. More than 2,000 small earthquakes in the range of 3.5–4.9 have occurred frequently, while, as the energy of seismic sources increases, the frequency of earthquakes decreases, with

fewer moderate events in the 5.0–6.4 range. Large earthquakes with magnitudes between 6.5 and 7.4 have occurred only nine times in total, providing important data for recurrence period and probability calculations.

Since the number of earthquakes (*N*) by magnitude shown in Table 1 supports the Gutenberg–Richter relationship, the logarithmic occurrence frequency and the data required for the magnitude–frequency distribution are presented in Table 2.

Table 2 lists the number of earthquakes that occurred between 1900 and 2024 according to their magnitudes, and presents the average magnitudes calculated for each group, providing the necessary data prior to conducting the Gutenberg–Richter analysis. In Table 2, *M* denotes the magnitude, *N* the number of earthquakes, *Xi* the average magnitudes, *Yi* the logarithmic frequency, *Xi-Yi* and *i*<sup>2</sup> the products required for regression analysis, and *n* counter the order in which *Xi* values are included in the regression.

Table 2 shows that as earthquake magnitude increases, the value of Yi = log(N/Tg), representing the annual logarithmic frequency, decreases. In an earthquake

catalog, the minimum magnitude at which events are fully and reliably recorded is referred to as the Minimum Magnitude of Completeness (*Mc*). Previous studies have noted that *Mc* values vary over time due to incomplete historical records and exhibit geographic heterogeneity, thus requiring the development of specific maps for each region (Wiemer and Wyss, 2000; Woessner and Wiemer, 2005). In this study, analysis of the number of earthquakes and the logN–M relationship indicated that the frequency distribution becomes more regular and consistent with the Gutenberg–Richter relationship for magnitudes above 5.0. Therefore, *Mc* was set to 5.0, and the *n counter* was defined as 5 for the magnitude intervals between 5.0–5.4

and 7.0–7.4. The annual earthquake frequencies for different magnitudes are presented in Figure 2.

As shown in Figure 2, the graph presents Xi as the average magnitudes and Yi as log(N/Tg), representing the annual logarithmic earthquake frequency. The completeness magnitude (Mc) was determined as 5.0, and examination of earthquakes with M>5.0 in the figure 2 shows that the logarithmic number of earthquakes decreases with increasing magnitude, as illustrated by the fitted linear regression curve. For accurate calculation of the parameters b and a in the Gutenberg–Richter relationship, only data above the Mc threshold should be used (Woessner and Wiemer, 2005).

Table 2. Summary table prior to Gutenberg-Richter analysis

M	3.5-3.9	4.0-4.4	4.5-4.9	5.0-5.4	5.5-5.9	6.0-6.4	6.5-6.9	7.0-7.5
1900*2024 Arası N	2102	597	323	124	28	5	6	3
Xi	3,7	4,2	4,7	5,2	5,7	6,2	6,7	7,2
Yi = log(N/Tg)	1,23	0,68	0,42	0,00	-0,65	-1,39	-1,32	-1,62
Xi * Yi	4,55	2,87	1,95	0,00	-3,68	-8,65	-8,81	-11,64
i^2	13,69	17,64	22,09	27,04	32,49	38,44	44,89	51,84
n sayacı				1	2	3	4	5
Xi' lerin toplamı	31							
Yi'lerin toplamı	-4,97							
Xi * Yi 'lerin toplamı	-32,78							
Xi^2 lerin toplamı	194,7							

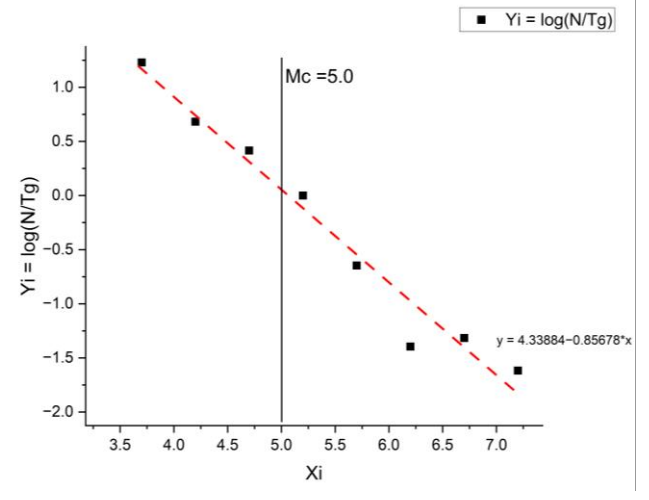


**Figure 2**. Annual Logarithmic Earthquake Frequency for Different Magnitudes

In Table 2, the total number of earthquakes by average magnitude, along with the sum of Xi, Yi, Xi. Yi, and  $Xi^2$  values, was obtained for the calculation of the "a" and "b" coefficients using the Least Squares Method (LSM). The formula for calculating the b coefficient

according to the Least Squares Method is given in Equation 4.

$$b = \frac{\sum XiYi - \frac{\sum Xi\sum Yi}{n}}{\sum Xi^2 - \frac{(\sum Xi)^2}{n}}$$

$$b = \frac{-32.78 - \frac{31* - 4.97}{5}}{194.7 - \frac{(31)^2}{5}}$$

$$b = -0.78$$

Using the Least Squares Method (LSM), the b coefficient was determined, and the a coefficient was calculated using Equation 5.

$$a = \frac{\sum Yi}{n} - b * \frac{\sum Xi}{n}$$

$$a = \frac{-4.97}{5} - (-0.722) * \frac{31}{5}$$

$$a = 3.84$$
(5)

The most widely known equation for magnitude—frequency distribution is the Gutenberg–Richter relationship, which, as shown in Equation 6, was applied by substituting the calculated *a* and *b* values to compute the results for each magnitude, subsequently illustrated in the figure 3 (Kalyoncuoğlu et al.).

### Log N(M) = 3.84 - 0.78M (6)

Table 3 presents the calculated logarithmic values based on the Gutenberg–Richter scale, showing that as earthquake magnitude increases, the corresponding logarithmic value rises proportionally. This indicates that larger earthquakes occur less frequently.

**Table 3**. Calculation of logarithmic values by magnitude

Magnitude	Formulation	Result
5.0	3.84-0.78*5	-0,058
5.5	3.84-0.78*5.5	-0,448
6.0	3.84-0.78*6	-0,838
6.5	3.84-0.78*6.5	-1,22
7.0	3.84-0.78*7	-1,61

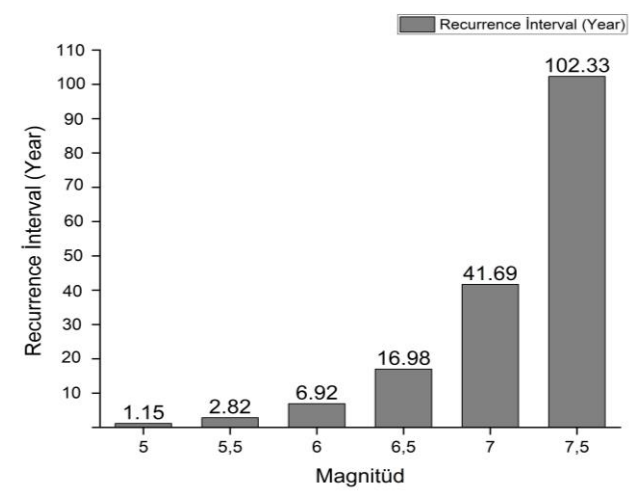


**Figure 3**. Graph of Earthquake Recurrence Times by Magnitude (in Years)

#### Calculation of earthquake recurrence periods

Within the framework of the Gutenberg–Richter scale, an instrumental period magnitude increment of  $\Delta M=0.1$  was adopted for the calculations. For this region, the relationship was determined as: logN(M)=3.84–0.78M

Accordingly, the recurrence time of earthquakes was calculated for each magnitude value using the formula:  $TR=\Delta T / 10(a-bMh)$ 

The calculated recurrence periods for each magnitude are presented in Table 4. Calculations of earthquake recurrence times indicate that an event with a magnitude of M = 5.0 occurs on average once every year or every 1–2 years, with a recurrence period of approximately 1.15 years. Statistically, this period increases with magnitude; for M = 7.0, the recurrence interval is estimated at approximately 30–50 years. For earthquakes of M = 7.5,

the recurrence period is calculated as approximately 102.33 years, indicating that events with magnitudes of 7.5 and 8.0 are rare occurrences with a frequency of more than once per century.

**Table 4**. Earthquake recurrence periods by magnitude (in Years)

Magnitu de	5	,5	6	,5 <sup>6</sup>	7	<b>7</b> ,
Recurren ce Time (Years)	,15	,82	,92	1 6,98	4 1,69	1 02,33

## Probabilities of earthquake occurrence within target periods

In seismic hazard analyses, the magnitude of earthquakes and their probabilities of occurrence within specific time frames are calculated. For instance, the probability of an earthquake with M = 5.0 occurring within 10 years is very high (99.98%), whereas the probability for an M = 7.0 event within the same period is relatively low (21.33%). It is evident that as earthquake magnitude increases, the probability of occurrence decreases, which is inversely proportional to the recurrence period.

These evaluations are highly significant for engineering structures and disaster management. Therefore, to investigate the likelihood of earthquakes occurring within specific periods, recurrence intervals of 10, 50, and 100 years were selected, and the probabilities were calculated using the formula: R=1-e-N(Mh)T

The results are presented in Table 5 and graphically illustrated in Figure 4.

Based on the seismic hazard analysis results:

- For earthquakes of magnitude 5.0 and 5.5, the probability of occurrence within 10 years ranges between 97.12% and 99.98%, while the probabilities within 50 and 100 years reach 100%.
- For earthquakes of magnitude 6.0 and 6.5, the probability of occurrence within 10 years ranges between 44.50% and 76.43%, within 50 years between 99.93% and 94.73%, and within 100 years between 100.00% and 99.72%.
- For earthquakes of magnitude 7.0 and 7.5, the probability of occurrence within 10 years ranges between 21.33% and 9.31%, within 50 years between 69.86% and 38.65%, and within 100 years between 90.92% and 62.36%.

The magnitudes and locations of historical earthquakes are consistent with the results of the seismic hazard analysis presented above. In conclusion, Western Turkey and the Aegean Region can be considered a seismic risk zone where multiple active faults, high deformation rates, weak soil conditions, and structural vulnerability intersect. Accurate analysis of this risk and its comparison across different scales is critically important for the development of region-specific disaster management strategies.

Table 5. Earthquake magnitudes and probability percentages based on seismic hazard analysis results

Magnitude	5	5,5	6	6,5	7	7,5
Probability of Occurrence Within 10 Years (%)	99,98%	97,12%	76,43%	44,50%	21,33%	9,31%
Probability of Occurrence Within 50 Years (%)	100,00%	100,00%	99,93%	94,73%	69,86%	38,65%
Probability of Occurrence Within 100 Years (%)	100,00%	100,00%	100,00%	99,72%	90,92%	62,36%

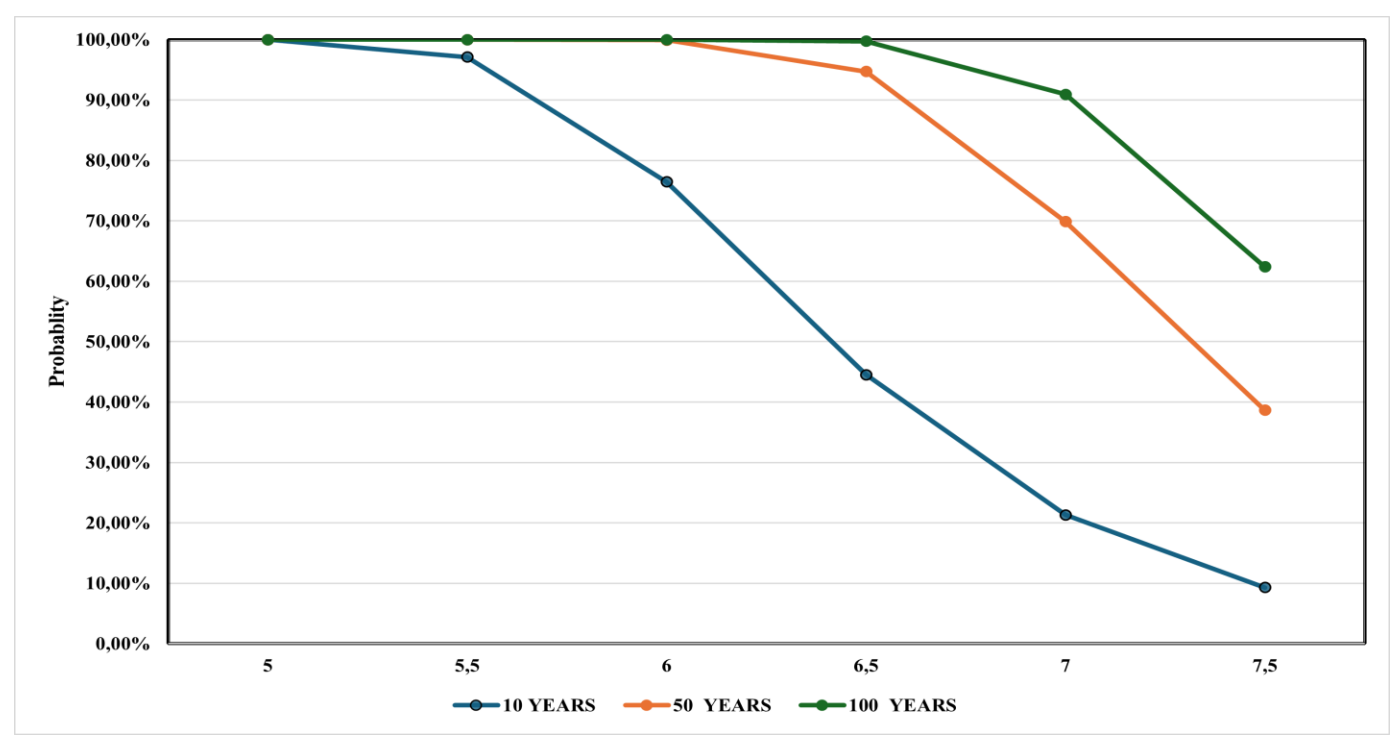


Figure 4. Graph of Earthquake Magnitudes and Probability Percentages Based on Seismic Hazard Analysis Results

#### CONCLUSIONS AND RECOMMENDATIONS

This study evaluated the seismotectonic framework of Turkey and the Aegean Region using historical and contemporary data. The analysis shows that Western Turkey faces high seismic risk due to intense crustal deformation and the complexity of fault systems. İzmir, Muğla, Balıkesir, and the Northern Aegean lie at the intersection of normal and strike-slip faults, where GPS and tomography data indicate heterogeneous deformation (Briole et al., 2021; Müller et al., 2013). Areas with elevated microseismic activity require continuous monitoring, as events such as the 2020 Samos–İzmir earthquake demonstrated the potential for tsunami

generation by offshore faults (Triantafyllou et al., 2021). Structural assessments reveal that much of the regional building stock is seismically inadequate. Infill walls, although non-structural, adversely affect overall performance and increase collapse risk (Aktaş et al., 2022). Historical earthquake data correspond closely with active fault maps and support the prediction of future seismicity (Denli, 2018). Seismic hazard analysis indicates the following probabilities within 50 years: M≥5.0 (100%), M $\geq$ 6.0 (99.9%), M $\geq$ 6.5 (94.7%), M $\geq$ 7.0 (69.9%), and M≥7.5 (38.7%). These results confirm the need for enhanced microseismic monitoring, updated hazard mapping, tsunami early warning systems, and structural retrofitting programs.

Overall, the findings provide a scientific basis for regional disaster risk reduction and evidence-based policy development.

#### **DECLARATIONS**

#### Corresponding author

Correspondence and requests for materials should be addressed to ; E-mail: Kyildirim@adu.edu.tr ; ORCID: https://orcid.org/0000-0002-7470-2297

#### Data availability

The datasets used and/or analysed during the current study available from the corresponding author on reasonable request.

#### **Supplementary Information**

The online version contains supplementary material available at link or upon request from the corresponding author.

#### **Competing interests**

The authors declare no competing interests in this research and publication.

#### REFERENCES

- Aktaş, Y. D., Ioannou, I., Malcıoğlu, F. S., Vatteri, A. P., Kontoe, M., Dönmez, K., ... & Diri-Akyıldız, F. (2022). Traditional structures in Turkey and Greece in the 30 October 2020 Aegean Sea earthquake: Field observations and empirical fragility assessment. Frontiers in Built Environment, 8, 840159. https://doi.org/10.3389/fbuil.2022.840159
- Anadolu Kılıç, N. C., & Kalyoncuoğlu, Ü. Y. (2017). Seismicity and seismic hazard analysis for Muğla province and its surroundings [Muğla ili ve çevresi için depremsellik ve sismik tehlike analizi]. *Journal of Engineering Sciences and Design*, 5(3), 507–524. https://doi.org/10.21923/jesd.348890
- Aslan, R. (2017). The 1957 Fethiye earthquake and its impacts on the region [1957 Fethiye Depremi ve bölgeye etkileri]. *Turkish Studies*, *12*(35), 33–47. <a href="http://dx.doi.org/10.7827/TurkishStudies.12645">http://dx.doi.org/10.7827/TurkishStudies.12645</a>
- Benetatos, C., Kiratzi, A., Ganas, A., Ziazia, M., Plessa, A., & Drakatos, G. (2006). Strike-slip motions in the Gulf of Siğaçik (western Turkey): Properties of the 17 October 2005 earthquake seismic sequence. *Tectonophysics*, 426(3–4), 263–279. https://doi.org/10.1016/j.tecto.2006.08.003
- Briole, P., Ganas, A., Elias, P., & Dimitrov, D. (2021). The GPS velocity field of the Aegean: New observations, contribution of the earthquakes, crustal blocks model. Geophysical Journal International, 226(1), 468–492. https://doi.org/10.1093/gji/ggab089

- Denli, Y. (2018). *Earthquakes in Turkey* (1928–1950) [Türkiye'de depremler (1928–1950)] (Master's thesis, Kafkas University). Thesis Link
- Ganas, A., Drakatos, G., Pavlides, S. B., Stavrakakis, G. N., Ziazia, M., Sokos, E., & Karastathis, V. K. (2005). The 2001 Mw = 6.4 Skyros earthquake: Conjugate strike-slip faulting and spatial variation in stress within the central Aegean Sea. *Journal of Geodynamics*, 39(1), 61–77. https://doi.org/10.1016/j.jog.2004.09.001
- Kalyoncuoğlu, Y., Uyanık, O., Altuncu, S., & Geçim, E. (2006). Gutenberg–Richter bağıntısındaki *b* değerinin tespiti için alternatif bir metot ve Güneybatı Türkiye'de bir uygulaması [An alternative method for the estimation of *b*-value in the Gutenberg–Richter relation with an application in southwest of Turkey]. *DEÜ Mühendislik Fakültesi Fen ve Mühendislik Dergisi*, 8(2), 67–78. Google Akademik
- Kılıç, M. (2006). Formation of the Gulf of İzmir: Evaluation of active faults controlling the gulf and the seismicity of the region in a GIS environment [İzmir Körfezi'nin oluşumu: Körfezi denetleyen aktif faylar ve bölgenin depremselliğine etkisinin GIS ortamında değerlendirilmesi] (Master's thesis). Dokuz Eylül University, Institute of Science, Department of Geological Engineering, Applied Geology Division, İzmir, Turkey. Google Akademik
- Müller, M. D., Geiger, A., Kahle, H.-G., et al. (2013). Velocity and deformation fields in the North Aegean domain, Greece, and implications for fault kinematics, derived from GPS data 1993–2009. *Tectonophysics*, 597–598, 34–49. https://doi.org/10.1016/j.tecto.2012.08.003
- Papanikolaou, D., Nomikou, P., et al. (2019). Active tectonics and seismic hazard in Skyros Basin, North Aegean Sea. *Marine Geology*, 407, 94–110. https://doi.org/10.1016/j.margeo.2018.10.001
- Pardo-Igúzquiza, E., & Dowd, P. A. (2024). Inference of the Gutenberg–Richter b-value: New insights and results. Tectonophysics, 890, 230486. https://doi.org/10.1016/j.tecto.2024.230486
- Seyrek, E. (2020). Evaluation of the new Turkey seismic hazard map for the Aegean region [Yeni Türkiye sismik tehlike haritasının Ege bölgesi için değerlendirilmesi]. NOHU Journal of Engineering Sciences, 9(1), 414–423. Google Akademik
- Sezer, L. İ. (2003). Earthquake activity and risk in the Muğla region [Muğla yöresinde deprem aktivitesi ve riski]. In *Proceedings of the IV Quaternary Workshop* (pp. 111–119). İstanbul: ITU Eurasia Institute of Earth Sciences. Google Akademik
- Tağıl, Ş. (2004). Neotectonic characteristics and seismicity of the Balıkesir Plain and its surroundings [Balıkesir Ovası ve yakın çevresinin neotektonik özellikleri ve depremselliği]. Journal of Geographical Sciences, 2(1), 73–92. <a href="https://doi.org/10.1501/Cogbil\_0000000038">https://doi.org/10.1501/Cogbil\_0000000038</a>
- Triantafyllou, I., Gogou, M., Mavroulis, S., Lekkas, E., Papadopoulos, G. A., & Thravalos, M. (2021). The tsunami caused by the 30 October 2020 Samos (Aegean Sea) Mw 7.0 earthquake: Hydrodynamic features, source properties, and impact assessment. *Journal of Marine Science and Engineering*, 9(1), 68. https://doi.org/10.3390/jmse9010068

- Wiemer, S., & Wyss, M. (2000). Minimum magnitude of completeness in earthquake catalogs: Examples from Alaska, the Western United States, and Japan. *Bulletin of the Seismological Society of America*, 90(4), 859–869. https://doi.org/10.1785/0119990114
- Woessner, J., & Wiemer, S. (2005). Assessing the quality of earthquake catalogues: Estimating the magnitude of completeness and its uncertainty. *Bulletin of the Seismological Society of America*, 95(2), 684–698. <a href="https://doi.org/10.1785/0120040007">https://doi.org/10.1785/0120040007</a>
- Yerli, B., Softa, M., & Sözbilir, H. (2021). Gümüldür Fayının morfometrik ve kinematik analizi ve Batı Anadolu'daki sismotektonik anlamı [Morphometric and Kinematic

- Analysis of Gümüldür Fault and Its Seismotectonic Implications for Western Anatolia]. *Türkiye Jeoloji Bülteni*, 64(2021), 349–382. https://doi.org/10.25288/tjb.846813
- Yıldırım, B. (2016). Neotectonic investigation of the southeastern Aegean Sea in light of the Marmaris, Yeşilova, and Gökova earthquakes [Marmaris, Yeşilova ve Gökova depremleri ışığında Güneydoğu Ege Denizi'nin neotektonik incelenmesi] (Master's thesis). Dokuz Eylül University, Institute of Science, Department of Marine Sciences and Technology, Marine Geology and Geophysics Program, İzmir, Turkey. Google Akademik

**Publisher's note:** Scienceline Publication Ltd. remains neutral with regard to jurisdictional claims in published maps and institutional affiliations.

Open Access: This article is licensed under a Creative Commons Attribution 4.0 International License, which permits use, sharing, adaptation, distribution and reproduction in any medium or format, as long as you give appropriate credit to the original author(s) and the source, provide a link to the Creative Commons licence, and indicate if changes were made. The images or other third party material in this article are included in the article's Creative Commons licence, unless indicated otherwise in a credit line to the material. If material is not included in the article's Creative Commons licence and your intended use is not permitted by statutory regulation or exceeds the permitted use, you will need to obtain permission directly from the copyright holder. To view a copy of this licence, visit <a href="https://creativecommons.org/licenses/by/4.0/">https://creativecommons.org/licenses/by/4.0/</a>.

© The Author(s) 2025